Adsorption 5, 229–244 (1999)

A General Package for the Simulation of Cyclic Adsorption Processes

FRANCISCO A. DA SILVA, JOSÉ A. SILVA AND ALÍRIO E. RODRIGUES*
Laboratory of Separation and Reaction Engineering, Faculty of Engineering, University of Porto, 4099 Porto Codex, Porto, Portugal
arodrig@fe.up.pt

Received June 4, 1998; Accepted August 10, 1998

Abstract. A general purpose package for simulation of fixed-bed and cyclic adsorption processes (PSA/VSA and TSA) has been developed. The package allows various models options depending on combinations of conservation equations: Equilibrium model, Macropore or Micropore model (LDF model), Bidisperse model (double LDF model). The fluid flow follows Ergun's equation locally and the operation of the column can be isothermal, adiabatic or non-isothermal, non-adiabatic. Two important industrial separation processes are considered: the propylene/propane and the *n*/iso paraffins systems. A three-step TSA and a four-step VSA are considered for propylene/propane mixture while a four-step PSA and two-step adsorption/purge-desorption processes are applied to the *n*/iso paraffins separation.

Keywords: cyclic adsorption simulator, PSA, VSA, TSA, bulk separation, fixed-bed

Introduction

The modeling of cyclic adsorption processes such as Pressure Swing Adsorption (PSA), Vacuum Swing Adsorption (VSA) and Temperature Swing Adsorption (TSA) requires the simultaneous solution of partial differential equations coupled with algebraic equations. Analytical solutions of the mathematical model are only available when approximations are used; otherwise, numerical solutions should be employed. Commercial simulation packages are well established for steady state problems. However, only recently, dynamic process simulators specially dedicated for solving general cyclic adsorption problems have appeared. LaCava et al. (1989) developed DAPS (Dynamic Adsorption Process Simulator) used to simulate a PSA plant for nitrogen production under isothermal operation without pressure drop in the column. Tidball et al. (1989) developed ADSIM/SU which offers a wide spectrum of model and operating conditions for a pre-defined adsorption process as: fixed-bed, two-bed PSA, one single Rapid PSA, two-bed TSA and three-bed VSA. Chlendi (1993) developed PSASIM, which allows the study of isothermal PSA processes with negligible pressure drop, with the possibility to include multiple adsorbents per column and until 20 steps for defining the process. Kumar et al. (1994), introduced SIMPAC, which presents several equilibrium isotherm options, a linear driving force (LDF) for the mass transfer model and an overall single energy balance and takes into account the pressure drop along the column through Ergun's equation. They tested the simulator to represent the recovery/purity of N_2-PSA, H_2-PSA and O_2-VSA processes. Liu and Ritter (1996) developed a four-step PSA simulator for studying the recovery of solvent vapor in non-isothermal non-adiabatic conditions, with LDF approximation, for two components and without pressure drop effect across the column. Malek and Farooq (1997) used a six-bed PSA of 10 steps for performing hydrogen recovery supported by pilot plant experiments; the simulator runs on a Cray916J supercomputer with parallel vector processing for solving the model.

In this work, the main objective is to present a general purpose package for the simulation of fixed-bed and cyclic adsorption processes as PSA/VSA and

*To whom correspondence should be addressed.

TSA working over a wide range of operating conditions. The simulator is not previously tailored for solving a specific cyclic adsorption process nor requires a special hardware for running. The package allows the choice between different models as: Equilibrium Model, Macropore Control model, Micropore Control model or Bidisperse Control using the LDF approach to characterize both the macropore or/and the micropore scale respectively. The process could be isothermal, adiabatic or non-isothermal or non-adiabatic and considers the pressure drop along the column through the solution of the Ergun's relationship for determining the superficial velocity locally. Various multicomponent equilibrium models are available and the package supports the combination of pressurization, feed and blowdown steps defined in sequential manner by the user, using the one-column bed approach to simulate the real multicolumn process (Kumar et al., 1994; Yang, 1987).

The package is tested for two important separation processes of industrial interest, in bulk separation conditions, namely propylene/propane system through a TSA and VSA processes and normal/iso paraffins mixtures with a PSA and adsorption/purge-desorption process. Finally, the usefulness of the package is verified by comparing simulated results with experimental data.

Mathematical Model

The mathematical model is based on the following assumptions:

(i) The gas phase follows the ideal gas law;
(ii) There are negligible mass, velocity and temperature gradients in the bed radial direction;
(iii) The linear driving force model (LDF) applies for representing the mass transfer inside the sorbent, at the crystal level and/or pellet scale;
(iv) Constant cross section, uniform void fraction and sorbent properties along the column;
(v) Ergun's equation is valid locally and the gas flow is subsonic;
(vi) The process can be isothermal, adiabatic or non-isothermal, non-adiabatic. The temperature is homogeneous inside the pellet.

The available models are ordered in four categories: Equilibrium Model, Macropore-Controlled Model, Micropore-Controlled Model and Bidisperse Model. Conservation equations common to all these categories are the overall mass balance in the bulk gas phase, the mass balance for each component in the bulk gas phase and the steady-state momentum equation as follows:

Overall Mass Balance

$$\varepsilon \frac{\partial C}{\partial t} = -\frac{\partial (uC)}{\partial z} - \sum_{i=1}^{n} N_i \tag{1}$$

where ε is the bed void fraction, C is the total molar concentration in the bulk phase, u is the superficial velocity, N_i is the molar volumetric flux of the "i" component exchanged between the solid phase and the bulk gas phase, constituted by "n" components.

The mass balance for each component at the bulk gas phase is written as:

Component Mass Balance

$$\varepsilon \frac{\partial C_i}{\partial t} = \frac{\partial}{\partial z}\left(\varepsilon D_{\mathrm{zm},i} C \frac{\partial Y_i}{\partial z}\right) - \frac{\partial (uC_i)}{\partial z} - N_i \tag{2}$$

where C_i is the mole concentration for the single component, $D_{\mathrm{zm},i}$ is the axial dispersion coefficient for the "i" component and Y_i is the mole fraction. Finally, the momentum equation represented by the Ergun's equation is written as:

Ergun's Equation

$$-\frac{\partial P}{\partial z} = \frac{150\mu(1-\varepsilon)^2}{\varepsilon^3 d_{\mathrm{p}}^2} u + \frac{1.75(1-\varepsilon)\rho}{\varepsilon^3 d_{\mathrm{p}}} |u|\, u \tag{3}$$

where P is the local pressure at z axial coordinate, μ is the gas viscosity, d_{p} is the pellet diameter and ρ is the gas density.

The definition of the N_i term is written in terms of the specific model considered as following:

(i) *Equilibrium Model*

$$N_i = (1-\varepsilon)\left(\varepsilon_{\mathrm{p}} \frac{\partial C_i}{\partial t} + \rho_{\mathrm{p}} w_{\mathrm{c}} \frac{\partial \bar{\bar{n}}_i}{\partial t}\right) \tag{4}$$

$$\bar{\bar{n}}_i = n_i^*(C_i, T_{\mathrm{s}}, P_{\mathrm{s}}) \tag{5}$$

where ε_{p} is the pellet porosity, ρ_{p} is the pellet density, w_{c} is the crystal weight fraction of the

pellet, $\bar{\bar{n}}_i$ is the average adsorbed mole concentration of the single component "i" per unit mass of the solid. The term n_i^* is the equilibrium value of the single component "i" evaluated with the bulk mole concentration C_i, temperature T_s and pressure P_s inside the pellet.

(ii) *Micropore Model*
In this case the Eq. (4) is used for defining N_i coupled with a mass balance around the crystal,

$$\frac{\partial \bar{\bar{n}}_i}{\partial t} = \frac{15\bar{D}_{c,i}}{r_c^2}(n_i^* - \bar{\bar{n}}_i) \tag{6}$$

$$n_i^* = n_i^*(C_i, T_s, P_s) \tag{7}$$

where Eq. (7) is a LDF type equation with $\bar{D}_{c,i}$ as the crystal diffusivity of the "i" component and r_c the crystal radius.

(iii) *Macropore Model*
The mole volumetric flux N_i term is defined as

$$N_i = (1-\varepsilon)\frac{aK_{m,i}}{(Bi_{m,i}+1)}(C_i - \bar{c}_i) \tag{8}$$

which is coupled to the mass balance around the pellet:

$$\frac{\partial \bar{c}_i}{\partial t} = \frac{15\bar{D}_{p,i}Bi_{m,i}}{R_p^2(Bi_{m,i}+1)}(C_i - \bar{c}_i) - \frac{\rho_p w_c}{\varepsilon_p}\frac{\partial \bar{\bar{n}}_i^*}{\partial t} \tag{9}$$

$$\bar{\bar{n}}_i^* = n_i^*(\bar{c}_i, T_s, P_s) \tag{10}$$

where a is external area per unit volume of the pellet, $K_{m,i}$ is the external mass transfer coefficient, $\bar{c}_i$ is the average mole concentration of the component "i" inside the pellet, $Bi_{m,i} = R_p K_{m,i}/(5\varepsilon_p \bar{D}_{p,i})$ is the mass Biot number and $\bar{D}_{p,i}$ is the pellet diffusivity.

(iv) *Bidisperse Model*
This model option is defined by the simultaneous solution of Eqs. (6), (8), (9) and (10), since both mass transfer resistances are coupled in series.

The set of equations just described is solved when the isothermal operation of the column is a valid assumption. When the thermal effects are not negligible, two kinds of energy balances are available:

Homogeneous Energy Balance

This energy balance assumes instantaneous temperature equilibrium between the gas, solid and wall shell of the column ($T_g = T_s = T_w$) written as:

$$\left\{\varepsilon C\tilde{C}_v + (1-\varepsilon)\left[\varepsilon_p \sum_{i=1}^{n}\bar{c}_i\tilde{C}_{v,i} + \rho_p w_c \sum_{i=1}^{n}\bar{\bar{n}}_i\tilde{C}_{v,\text{ads},i} + \rho_p\hat{C}_{ps}\right] + \varepsilon_w\rho_w\hat{C}_{pw}\right\}\frac{\partial T}{\partial t}$$
$$= \varepsilon\Re T\frac{\partial C}{\partial t} + (1-\varepsilon)\varepsilon_p\Re T\frac{\partial \bar{c}}{\partial t} + \frac{\partial}{\partial z}\left(\lambda\frac{\partial T}{\partial z}\right)$$
$$-uC\tilde{C}_p\frac{\partial T}{\partial z} + \rho_b w_c\sum_{i=1}^{n}(-\Delta H_i)\frac{\partial \bar{\bar{n}}_i}{\partial t}$$
$$-\varepsilon_w\alpha_{w\ell}U(T - T_\infty) \tag{11}$$

where $\tilde{C}_v$ is the molar specific heat of the bulk gas mixture, $\tilde{C}_{v,i}$ is the molar specific heat of the gaseous component "i", $\tilde{C}_{v,\text{ads},i}$ is the molar specific heat of the component "i" adsorbed at the solid phase which is considered equal to $\tilde{C}_{v,i}$ (Sircar, 1985). The $\hat{C}_{ps}$ and $\hat{C}_{pw}$ are the mass specific heat of the solid and wall respectively, ε_w is the wall volume to gas-solid volume ratio, $\alpha_{w\ell}$ is the ratio of the logarithmic mean surface area of the column shell to the volume of the column wall, ρ_w is the wall density, $\Re$ is the universal gas constant, λ is the axial heat dispersion coefficient, ρ_b is the bulk density, ΔH_i is the isosteric heat of adsorption of the component "i" and U is the overall heat transfer coefficient between the column and the surroundings. This energy balance is coupled with the equilibrium model and macro/micro pore control model.

Heterogeneous Energy Balance

The heterogeneous energy balance splits the energy balances in the column in three different control volumes:

(i) *Energy Balance for the Gas Phase:*

$$\varepsilon C\tilde{C}_v\frac{\partial T_g}{\partial t} = \frac{\partial}{\partial z}\left(\lambda\frac{\partial T_g}{\partial z}\right) - uC\tilde{C}_p\frac{\partial T_g}{\partial z} + \varepsilon\Re T_g\frac{\partial C}{\partial t} - (1-\varepsilon)ah_f(T_g - T_s) - \frac{2h_w}{R_w}(T_g - T_w) \tag{12}$$

where h_f and h_w are the heat transfer coefficient between the gas and the solid and between the gas and the wall, respectively, and R_w is the column internal radius.

(ii) *Energy Balance for the Adsorbent*

$$(1-\varepsilon)\left\{\varepsilon_{\mathrm{p}}\sum_{i=1}^{n}\bar{c}_i\tilde{C}_{v,i}+\rho_{\mathrm{p}}w_{\mathrm{c}}\sum_{i=1}^{n}\bar{\bar{n}}_i\tilde{C}_{v,\mathrm{ads},i}+\rho_{\mathrm{p}}\hat{C}_{\mathrm{ps}}\right\}\frac{\partial T_{\mathrm{s}}}{\partial t}$$
$$=(1-\varepsilon)\varepsilon_{\mathrm{p}}\Re T_{\mathrm{s}}\frac{\partial\bar{c}}{\partial t}+\rho_{\mathrm{b}}w_{\mathrm{c}}\sum_{i=1}^{n}(-\Delta H_i)\frac{\partial\bar{\bar{n}}_i}{\partial t}+(1-\varepsilon)h_{\mathrm{f}}a(T_{\mathrm{g}}-T_{\mathrm{s}}) \quad (13)$$

(iii) *Wall Energy Balance*

$$\rho_{\mathrm{w}}\hat{C}_{\mathrm{pw}}\frac{\partial T_{\mathrm{w}}}{\partial t}=\alpha_{\mathrm{w}}h_{\mathrm{w}}(T_{\mathrm{g}}-T_{\mathrm{w}})-\alpha_{\mathrm{w}\ell}U(T_{\mathrm{w}}-T_{\infty}) \quad (14)$$

where α_w is the ratio of the internal surface area to the volume of the column wall (Huang and Fair, 1988).

The PSA cycle can include combinations of the following steps: pressurization, feed/purge and blowdown steps. It allows also the inclusion of equalization and waiting steps. For the feed/purge steps the Danckwerts boundary conditions are applied while for the pressurization/blowdown steps an exponential type equation is applied to the open end (Lu et al., 1993). In the case that internal product streams from other columns are required as input of foregoing steps (for example, purging with high purity product), the properties of the source stream are averaged and the total amount is stored along the time. Then, a fraction of this average output stream is introduced as feed for the required step (Sikavitsas et al., 1995).

The initial condition of the column can be of two forms: a closed column or open column with isothermal flow, in both cases saturated with an arbitrary fixed temperature, pressure and composition mixture. Once the simulation is started the final condition of the last step constitutes the initial condition of the following cycle.

The ideal adsorption model or IAS (Myers and Prausnitz, 1965), real adsorption model or RAS (Talu et al., 1995), the loading rate correlation or LRC (Yang, 1987), Nitta et al. (1984) and an extended Toth equation (Sircar, 1991) are available for representing the multicomponent equilibrium isotherms.

Molecular diffusivities are calculated with Chapman-Enskog equation and gas specific heat, gas viscosity and gas heat conductivities are temperature and pressure dependent, being calculated using the methods and thermodynamic data found in Reid et al. (1987). Molecular difusivities and viscosities of mixtures are calculated using Wilke rules (Bird et al., 1960), while pore diffusivities are calculated using Bosanquet relationship (Park et al., 1996). Mass and heat axial dispersion terms $D_{\mathrm{zm},i}$, λ, and the $K_{m,i}$ and h_{f} values are calculated using the following correlations (Wakao and Funazkri, 1978; Wakao and Chen, 1987; Yang, 1987):

$$\frac{\varepsilon D_{\mathrm{zm},i}}{D_{m,i}}=\gamma_1+\gamma_2 Sc_i Re \quad (15)$$

$$\frac{\lambda}{k_g}=\gamma_3+\gamma_4 Pr\,Re \quad (16)$$

$$Sh_i=2.0+1.1Re^{0.6}Sc_i^{1/3} \quad (17)$$

$$Nu=2.0+1.1Re^{0.6}Pr^{1/3} \quad (18)$$

and change along the column (Lu et al., 1993); $Sc_i=\frac{\mu}{\rho D_{m,i}}$ is the Schmidt number for the component "i", $Re=\frac{\rho u d_{\mathrm{p}}}{\mu}$ is the Reynolds particle number, $Pr=\frac{\hat{C}_{\mathrm{pg}}\mu}{k_{\mathrm{g}}}$ is the Prandl number, $\gamma_1=20, \gamma_2=0.5, \gamma_3=7$ and $\gamma_4=0.5$ while $\hat{C}_{\mathrm{pg}}$ is the local specific heat per kilogram at constant pressure and k_{g} is the thermal conductivity of the gas mixture.

Model Integration and Package Description

The model equations are arranged inside the numerical package, that we call SAXS (Swing Adsorption X = Pressure or Temperature Solver), in five blocks: three related with conservation equations (Mass, Energy and Momentum balances), one block dedicated to the calculation of the thermodynamic and equilibrium properties and one block where the initial and boundary conditions are implemented.

The bidisperse model based on the double LDF approach (Cen and Yang, 1989) combined with the heterogeneous energy balance (Huang and Fair, 1988), constitutes the more general model available in the package. The equilibrium model combined with the homogeneous energy balance (Lu et al., 1993) constitutes the simpler model available, while the Micropore controlled and Macropore controlled models plus the homogeneous energy balance are intermediate options. The model options directly available from the package are the Equilibrium, Macropore-controlled

and Micropore-controlled with Homogeneous Energy Balance and Bidisperse control with Heterogeneous energy balance; other possible options are available indirectly by introducing appropriate limiting parameters in the bidisperse/heterogeneous energy balance model. For example if a Macropore model with Heterogeneous Energy Balance is required, the user implements this particular case from the Bidisperse Model combined with Heterogeneous energy balance by introducing a negligible crystal resistance throughout the input parameters.

The simulation case is defined with three single text files: (a) Main File, where the model type, number of components, column and solid properties and numerical tolerances are introduced. (b) Properties file, where the critical, kinetics and equilibrium properties are defined by component and (c) Cycle definition file, where the initial conditions and process steps are defined. The simulator reports the solution through three files: at fixed equidistant points with the time as independent variable (history files), along the column at fixed intervals of time (axial profile files) and averaged mass flow in/out of the column (global mass balance files) for each step of process during all simulation. The simulation is followed with the graphics displaying all the variables until the profiles in a cycle are similar to those in the previous cycle. Then the global mass balance over the cycle is checked. When the simulation is stopped without satisfying the cyclic periodic condition, it can be re-started again from the previous state as initial condition.

Numerical Solution

The set of partial differential equations are first transformed in a dimensionless form (Da Silva et al., 1996) and the resulting system is solved using the method of lines (Schiesser, 1991). The spatial coordinate is discretized using the method of orthogonal collocation on finite elements (Carey and Finlayson, 1975). For the spatial dimension a minimum of 10 to 200 elements are used, with at least two internal collocation points for all the cases. The number of elements is established after consistent results are obtained by comparing simulated results from the equilibrium model and the more complete models at different grid densities until negligible deviations are found. For each element, the basis polynomial were calculated using the routines developed by Villadsen and Michelsen (1978), selecting the shifted Jacobi polynomials with weighting function $W(x) = 1(\alpha = 0, \beta = 0)$ that has equidistant roots inside each element. The total number of equations, including boundary conditions, algebraic equations and residual equations depends on the respective model solved as follows. If we define the number of finite elements as M, the number of internal collocation points as C and the number of mixture components as N, the total number of equations solved with the equilibrium model is $[M(C+1)+1](N+2)$, for the macro or micro pore control models is $[M(C+1)+1](2N+2)$ while for the bidisperse control model is $[M(C+1)+1](3N+4)$. For the isothermal cases, the $(N+2)$, $(2N+2)$ and $(3N+4)$ factors are reduced to $(N+1)$, $(2N+1)$ and $(3N+1)$ respectively. The total number of differential-algebraic equations solved for this work varies between 906 to 1592.

The set of discretized ordinary differential equations are then integrated with the DAE solver DASPK (Brown et al., 1994) which is based in a backward differentiation formulas. The relative and absolute tolerance were fixed at 10^{-4} and 10^{-5} respectively in double precision arithmetic for all calculated variables, with the exception of the superficial velocity which was solved with 10^{-3} for both tolerances. The code was written in C language and runs in any operative system with appropriated standard compiler. The simulations were ran in AIX RS6000, DEC-Alpha 3000 workstations and in Linux-PC boxes with Intel 586-166 MHz processor, spending between 5 to 20 CPU minutes per cycle, depending on the type of cycle, the model implemented and the load of the specific operating system. SAXS is a package oriented to personal computer and small workstations and its performance can be considered reasonable as compared to similar software applications.

Results and Discussion

Propylene/Propane Separation

The propylene/propane system is an energy consuming process which is targeted to be improved by combining the distillation technology with adsorption process (Kumar et al., 1992). The simulator is used to study the propylene/propane separation over a fixed-bed column and two cyclic adsorption processes in order to produce high purity propylene are considered. The TSA and VSA examples are just examples to illustrate the capabilities of the software.

Fixed-Bed Runs

The fixed-bed run is presented as a preliminary test of the simulator. Järvelin (1990) and Järvelin and Fair (1993) performed several experiments of fixed-bed adsorption/desorption in non-isothermal, non-adiabatic conditions of propylene/propane over different adsorbents. The better adsorbent choice was the zeolite 13X and additional multicomponent equilibrium and kinetics for the same system are taken from Huang et al. (1994) and Brandani et al. (1995). The experimental multicomponent equilibrium was fitted using the LRC correlation, taking into account the single component equilibrium found in Järvelin and Fair (1993), and single and multicomponent data reported by Huang et al. (1994). The fixed bed experimental multicomponent breakthrough reported by Järvelin and Fair (1993) was also taken into account to correct the multicomponent predictions of LRC correlation. The heat transfer coefficients h_w and U were taken from Schork and Fair (1988).

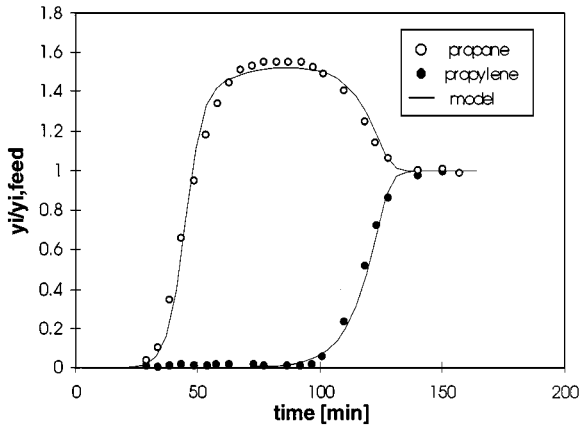

Figure 1. Multicomponent adsorption breakthrough of propylene/propane mixture on 13X zeolite. Points are experimental data from Järvelin and Fair (1993). Lines are model predictions with the bidisperse model and heterogeneous energy balance, operating in non-isothermal, non-adiabatic conditions.

The main operating conditions and parameters for the fixed-bed breakthrough runs over 13X zeolite are shown in Table 1. Figure 1 shows a simulated breakthrough curve with the bidisperse control model and the heterogeneous energy balance compared with the experimental data supplied by Järvelin and Fair (1993) for a multicomponent system propylene/propane/nitrogen. The multicomponent breakthrough shows the typical roll-up for the propane that is the less adsorbed species being displaced by the propylene. Figure 2 shows the propylene adsorption/desorption experiment reported by Järvelin (1990), for the same experimental set, operating in non-isothermal, non-adiabatic operating conditions with single propylene diluted with nitrogen, showing the experimental breakthrough and

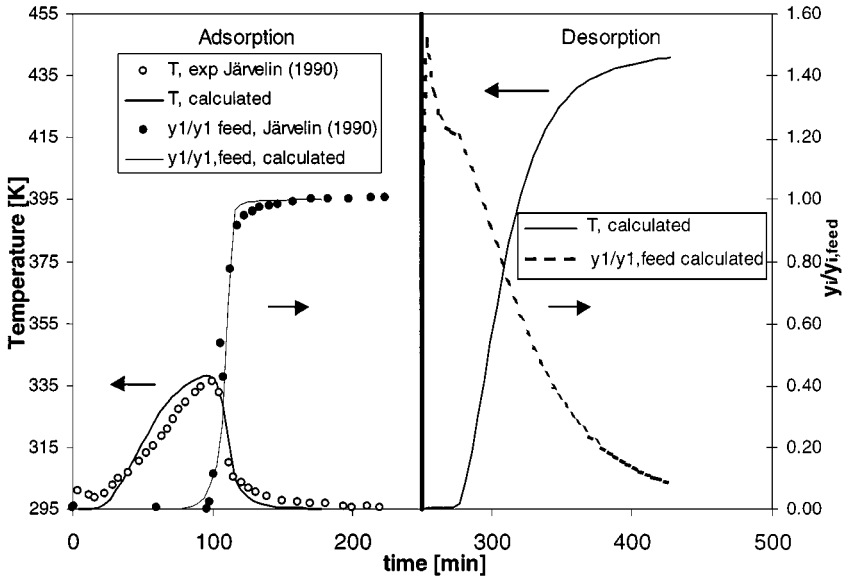

Figure 2. Propylene adsorption and desorption breakthrough on 13X zeolite. Temperature excursion is also shown. Points are experimental data from Järvelin (1990). Lines are model predictions with the bidisperse and heterogeneous energy balance, operating in non-isothermal, non-adiabatic conditions.

Table 1. Parameters for fixed-bed and TSA processes for propylene/propane separation.

Column:			
Bed length, L,		1.22	m
Internal radius, R_w,		4.24	cm
Bed porosity, ε,		0.395	—
Feed temperature, T_0,		296	K
Feed pressure, P_0,		269	kPa
Feed superficial velocity, u_o,		0.195	m/s
Molar feed composition,	C_3H_6 (1)	1.161	%
	C_3H_8 (2)	1.185	%
	N_2 (3)	97.654	%
Wall density, ρ_w,		8238	kg/m^3
Wall specific heat, $\hat{C}_{pw}$,		500	J/kg K
Wall heat film transfer, h_w,		40.3	W/m^{2}K
Overall heat transfer, U,		1.72	W/m^{2}K

Adsorbent: 13X zeolite.

Crystal radius, r_c,		1.0	μm
Pore radius, r_p,		0.17	μm
Pellet radius, R_p,		1.6	mm
Pellet density, ρ_p,		1140	kg/m^3
Pellet void fraction, ε_p		0.27	—
Bulk density, ρ_b,		690	kg/m^3
Tortuosity, τ,		6.0	—
Specific solid heat, $\hat{C}_{ps}$,		920	J/kg K

Equilibrium: LRC model.

$$n_i^* = m_i k_i P_i \chi_i \Big/ \left(1 + \sum_{i=1}^{n} k_i P_i \chi_i\right); \; m_i = A_i \exp(B_i/T) \quad k_i = C_i \exp(D_i/T)$$

Component	A_i (mol/kg)	B_i (K)	C_i (kPa^{-1})	D_i (K)	χ_i	$-\Delta H_i$ (J/mol)
Propylene	1.31	170.7	6.437 10^{-5}	2895.5	13.6	52777
Propane	0.495	353.9	3.252 10^{-5}	2826.4	3.72	46888

Crystal Diffusion Parameters:

$$\bar{D}_{c,i} \approx D_{oc,i} \exp(-E_i/\Re T)$$

Component	$D_{oc,i}$ (m^2/s)	E_i (J/mol)
Propylene	5.8 10^{-8}	23750
Propane	1.4 10^{-8}	21100

temperature history at the exit end of the column, being compared with the model simulations. In both cases model results compare fairly well with the experimental breakthrough data. Also shown are the simulated breakthrough and the desorption curve obtained with a hot purge stream of single nitrogen at 479 K with the same total molar flow introduced in the adsorption step.

TSA Process

The simulated TSA process has three steps: (i) Feed at 298 K with a equimolar mixture of propylene/propane diluted with nitrogen (10% propylene, 10% propane and 80% nitrogen); (ii) A cocurrent higher temperature purge step with nitrogen at 358 K; (iii) A lower temperature purge step with nitrogen in countercurrent

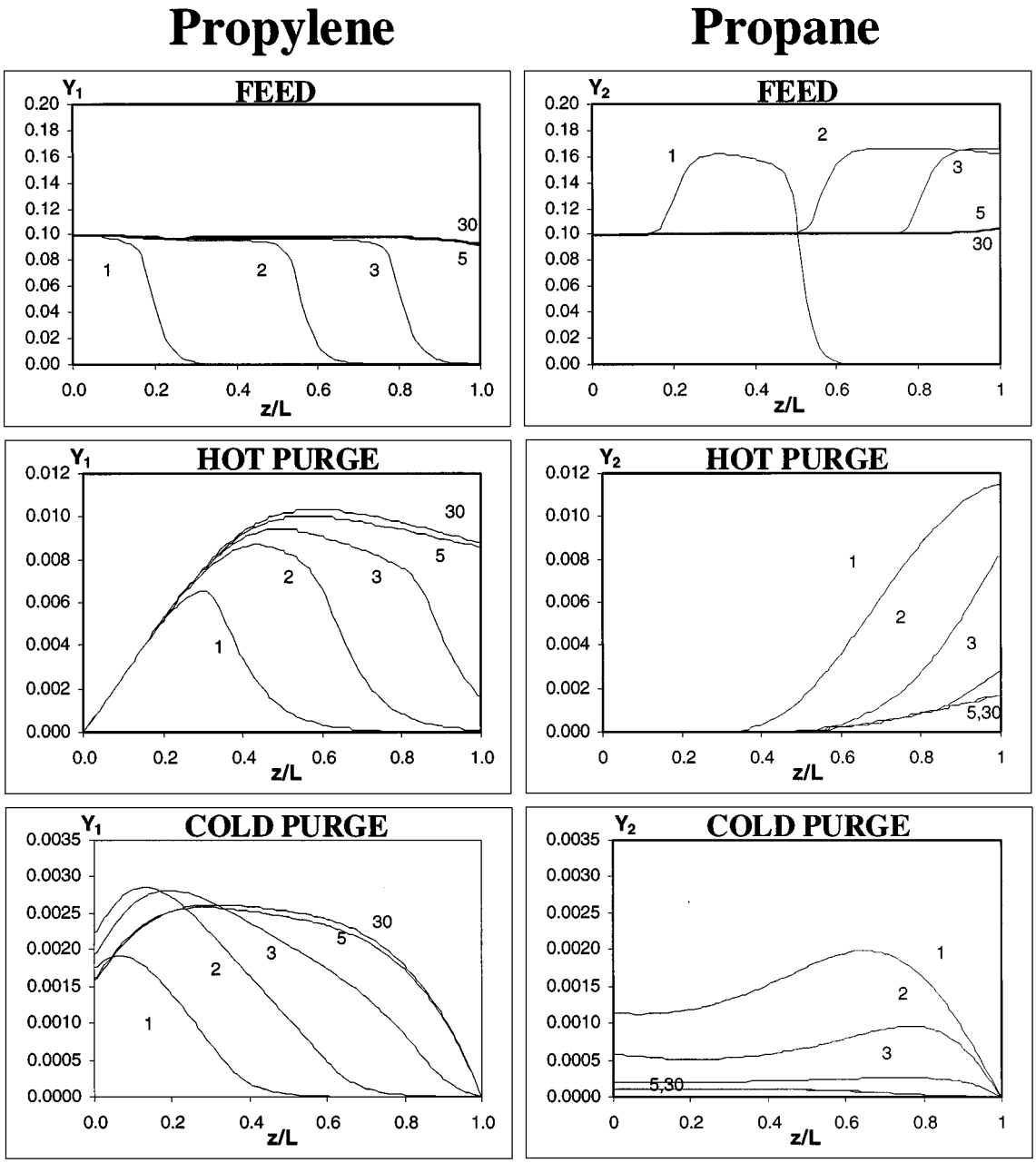

Figure 3. Mole fraction evolution for propylene and propane at bulk gas phase inside the column until the cyclic steady-state for the three-step TSA process based on the adsorption/desorption two-step process of Järvelin and Fair (1993), solving the bidisperse control model and heterogeneous energy balance, operating in non-isothermal, non-adiabatic conditions.

at 298 K, where single diluted propylene is obtained. The main operating parameters and the selected mathematical model are the same of the previous fixed-bed experiments with the following additional changes: the mole fraction of the propane/propylene feed mixture is incremented from near 3 to 20%, the column is now operating at atmospheric pressure with 1 m length and 8 cm diameter. The column is initially filled with nitrogen at 101 kPa and 298 K. All three steps spent 16 min each working with a loading of 522 L/h kg cycle at standard conditions (273 K, 101 kPa).

For this TSA process the hot temperature was kept well below to 473 K for the following reasons: (a) to avoid extrapolating the experimental data from the temperature for which the original parameters are defined (between 296 and 358 K); (b) to avoid form coking over 13X zeolite due to the presence of propylene in the feed mixture which is further incremented during the purge step; (c) to have a shorter TSA cycle.

Figure 3 shows the mole fraction of propylene and propane at the end of each step where mole fraction profiles are practically identical between the cycle 5 to 30. During the feed step, the typical wave motion of the more adsorbable component (propylene) and the roll-up of the less adsorbable species (propane) is displayed. During the hot purge step, the column is practically cleaned of propane until near the half of the column during the first cycle, and then progressively along almost all the column, while the propylene is arriving at the exit end during the hot purge step. The cold countercurrent step shows that after the third cycle, a high purity propylene stream relative to propane in free nitrogen base is obtained.

Figure 4 shows the evolution of temperature profiles from the first step until the steady state conditions at the end of each step. In the feed step two temperature maxima are detected as consequence of two mass transfer zones that occur during the adsorption step. The first from right to left, is the result of propane which is re-adsorbed after being desorbed from the second mass transfer zone, as consequence of being displaced by the propylene which is the more adsorbed component. Then, after the second cycle, the breakthrough of propane occurs and the first mass transfer zone disappears at the end of the feed step. The second temperature peak also moves until leaving at the exit end as consequence of the propylene breakthrough. The cyclic steady state temperature profile is then achieved more as a consequence of mixture between hot/cold streams in the column than because of heat adsorption/desorption effects. During the hot purge steps the temperature wave evolution is coupled with mass transfer zone of propylene until occurs the breakthrough. Then during the cold purge when the pure nitrogen is entering from right to left, the axial profile shows the characteristic depression which follows the purge desorption steps.

The numerical solution used 30 finite elements with 2 internal collocation points. Nearly 30 cycles are needed to achieve the steady state conditions and the computer time is 18–22 CPU min by cycle simulated.

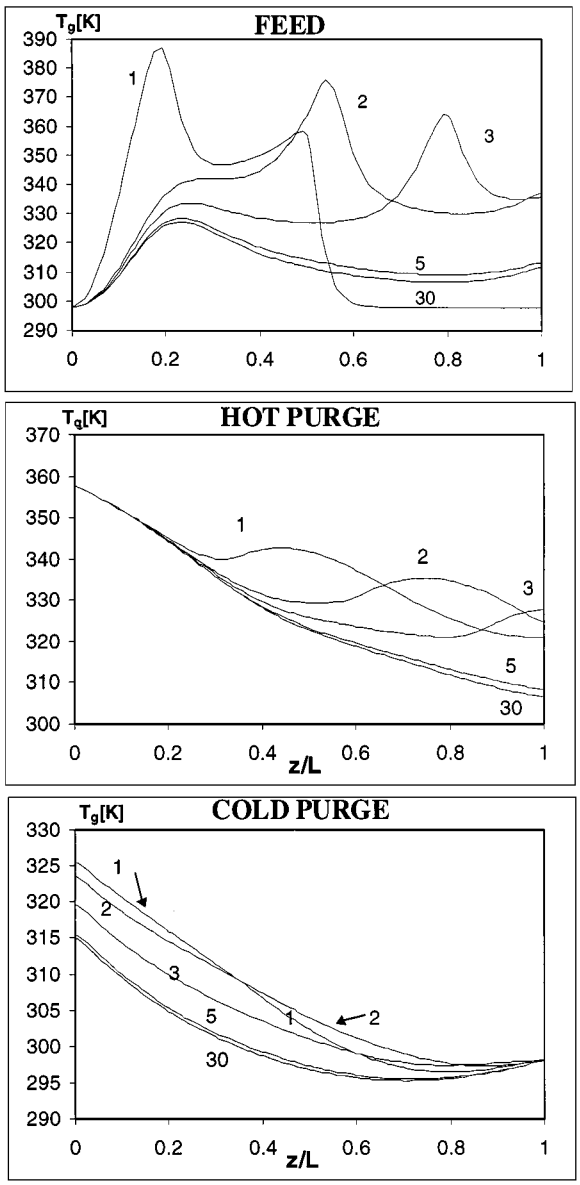

Figure 4. Axial gas temperature evolution inside the column until the cyclic steady-state for the three-step TSA process.

VSA Process

A second cyclic process considered for separating the propylene/propane is a four-step VSA. The main advantage of pressure swing over temperature swing during adsorption/desorption process is the possibility to work with shorter cycles and achieve faster the cyclic state steady-state. Additionally, the possibility to form

Table 2. Main operating parameters for the VSA process for the propylene/propane separation.

Column:			
Bed length, L,		3.5	m
Tube inside radius, R_w,		100	cm
Bed porosity, ε,		0.4	—
Wall density, ρ_w,		8238	kg/m^3
Wall specific heat, $\hat{C}_{pw}$,		500	J/kg K
Wolar feed composition,	C_3H_6 (1)	48	%
	C_3H_8 (2)	52	%
Adsorbent: Amberlyst 15 Ag^+—Resin.			
Pellet radius R_p,		0.3	mm
Bulk density, ρ_b,		670	kg/m^3
Specific solid heat, $\hat{C}_{ps}$,		1170	J/kg K

Equilibrium: LRC model

$$n_i^* = m_i k_i P_i \chi_i \Big/ \left(1 + \sum_{i=1}^{n} k_i P_i \chi_i\right); \; m_i = A_i \exp(B_i/T) k_i = C_i \exp(D_i/T)$$

Component	A_i (mol/kg)	B_i (K)	C_i (kPa^{-1})	D_i (K)	χ_i	$-\Delta H_i$ (J/mol)
Propylene	0.351	354.2	$1.28\ 10^{-2}$	886.0	1.0	43054
Propane	$9.0\ 10^{-5}$	2401.8	$0.268\ 10^{-2}$	397.0	1.0	21318

Micropore Diffusion Parameters:

$15 D_{c,i}/r_c^2 \approx$ constant

Component	$15 D_{c,i}/r_c^2$ (s^{-1})
Propylene	$1.2\ 10^{-5}$
Propane	$4.0\ 10^{-5}$

coke in the presence of propylene in the feed is decreased. The main limitation is the difficulty to regenerate the column during the blowdown step when the more adsorbed compound is the desired product as in the propylene/propane case considered here. The VSA process with 13X zeolite at lower temperature is not feasible due to the high irreversible behavior of the propylene isotherm at lower temperatures (Da Silva et al., 1996). A promising adsorbent with better equilibrium characteristics at low temperatures based on the π-complexation bonds between the Ag^+ exchanged resin and olefins have been developed by Yang and Kikkinides (1995). A VSA process with the operating conditions and experimental data from Sikavitsas et al. (1995) and the micropore controlled model is employed and the adiabatic operating condition is imposed.

The four-step VSA considered includes: (i) Pressurization with the feed mixture (48% mole propylene, 52% mole propane); (ii) Feed at high pressure with the fresh feed as in step (i) mixed with a recycle stream coming from the column performing purge step; (iii) Purge with part of the blowdown product at high pressure; (iv) Countercurrent blowdown step to vacuum, where the propylene high purity product is withdrawn. The main operating conditions employed are in Table 2. The column is initially filled with pure propylene at 101 kPa and 298 K and all the three steps have 40 min duration each. The feed loading per cycle is of 96.6 L/h kg at standard conditions (273 K, 101 kPa). High pressure of 101 kPa is kept during the first 3 steps at the feed end while the low pressure is kept at 5 kPa. Purge is performed at high pressure with feed averaged properties of the stream obtained as propylene high purity product during the blowdown step.

The numerical solution for this case requires 50 finite elements with two interior collocation point and nearly 100 cycles are needed to achieve the cyclic steady-state, with 5 to 8 CPU min per cycle. Figure 5 shows the mole fraction of propylene, superficial velocities, pressure and gas temperature histories at the middle of the column during the steady state conditions (the time scale was arbitrarily reset to 0). The propylene mole fraction history at the middle of the column can be understood as follows. During the pressurization step, the average mole fraction of propylene is nearly constant at 0.2. Then, during the feed step the gas flowing with

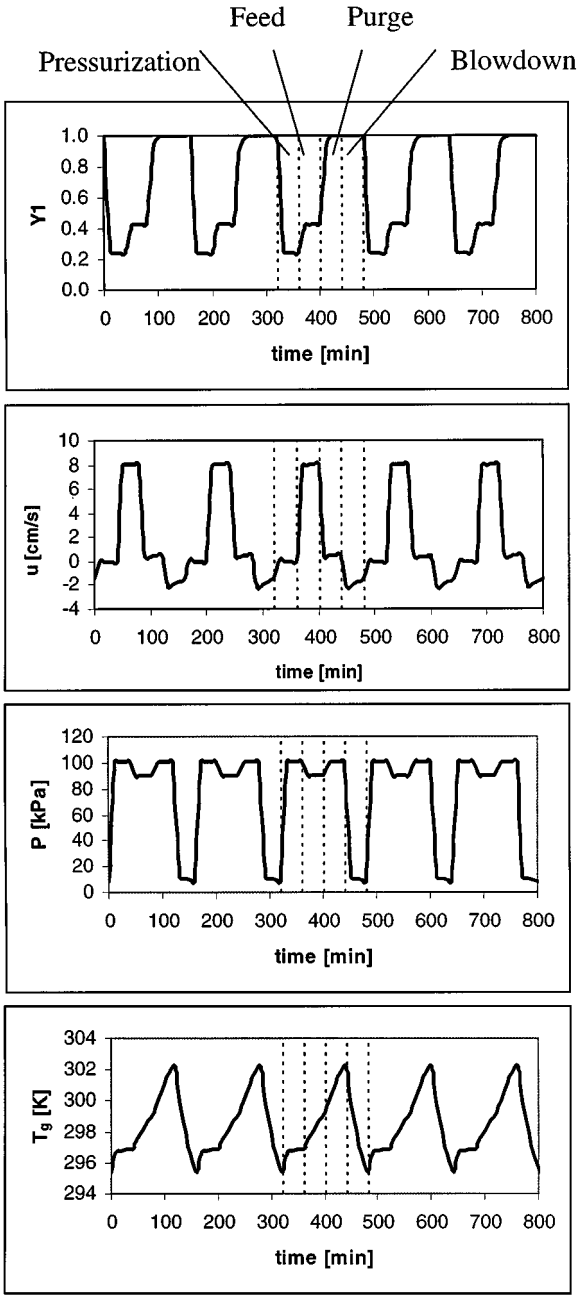

Figure 5. Mole fraction, superficial velocity, pressure and temperature histories at the middle of the column, during the cyclic steady-state VSA process, solving the micropore model with homogenous energy balance in adiabatic conditions.

the feed composition crosses the middle of the column (0.42 mole fraction of propylene) and then during the purge with high propylene product, the mole fraction rises progressively to nearly one. The cycle is closed with countercurrent blowdown step where the pressure is reduced to a low vacuum pressure level while the propylene mole fraction is kept nearly to one along all this period. Finally, during the beginning of the next pressurization step, the mole fraction of propylene drops faster to 0.2, beginning of the new cycle. An equivalent four-step path can be followed in the other graphs shown in Fig. 5 for the other variables. It is interesting to indicate two additional characteristics of this simulation. First, the pressure drops in the middle of the column from nearly 100 kPa at the end of the pressurization step to nearly 90 kPa at high pressure feed as a result of the strong adsorption occurring in this step (Arumugam and Wankat, 1996). Second, there is a temperature drop which follows the pressure decrease during blowdown as it is expected during a desorption step, when the more adsorbed component is desorbed from the solid phase.

Figure 6 compares the recovery versus purity curves for the TSA and VSA processes studied. From both methods it is possible to get high purity propylene as product (>99.5%); however, in both cases the recovery obtained is very low (between 2 and 14%). With the TSA alternative, a high purity propylene product relative to propane is obtained but diluted with inert gas (0.23% molar in nitrogen); therefore an additional separation step for recovering the nitrogen to be recycled to the system (Järvelin and Fair, 1993) is required. The simulated VSA process has a long cycle time in order to obtain a high quality propylene product as a consequence of high mass transfer resistances found for propylene and propane on the resin. Sikavitsas et al. (1995) obtained similar results using a particle diameter

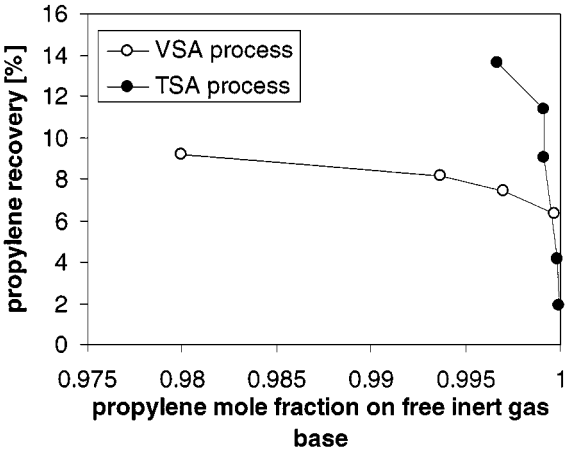

Figure 6. Propylene recovery vs propylene mole fraction on free inert gas base for the TSA and VSA processes.

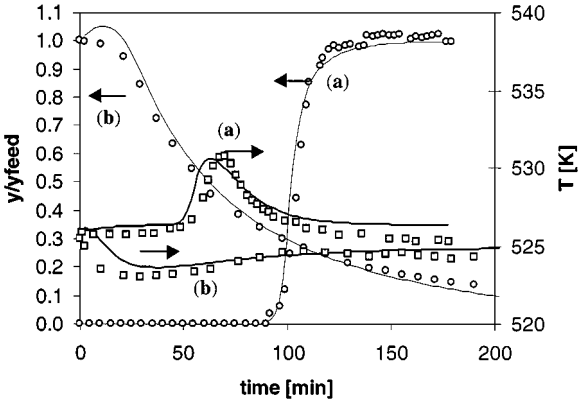

Figure 7. Adsorption (a) and countercurrent desorption (b) curves of *n*-pentane and temperature histories at z/L = 0.6 for the mixture of *n*/iso-pentane/N_2 over 5A zeolite. Experimental data of Silva and Rodrigues (1997). Lines are model predictions with the macropore model and homogeneous energy balance, operating in non-isothermal, non-adiabatic conditions.

of 0.6 mm but recoveries lower than 1%. However, using a 0.3 mm resin as introduced here has the drawback that larger pressure drops are obtained (8 kPa with 0.6 mm sorbent while with 0.3 mm sorbent particles a pressure drop of 24 kPa is obtained on the adsorption step), limiting its industrial applicability when used for VSA operations.

Normal/Iso Paraffins Separation

The *n*/iso paraffins has industrial importance for the improvement of the octane number of gasoline pools. A well known isomerization process used for obtaining high-octane branched isomers is total isomerization process (TIP) (Holcombe, 1980), where non reacting isoparaffins are recycled to the reactor. The n/iso paraffins separation is then performed using 5A zeolite as adsorbent.

Fixed-Bed Runs

The equilibrium adsorption isotherms and kinetic data for n-pentane and n-hexane on 5A zeolite were obtained with the gravimetric and ZLC techniques (Silva and Rodrigues, 1997a, 1997b). Kinetic data for this system shows that macropore diffusion is the controlling mechanism for mass transfer inside the adsorbent. Fixed-bed experiments with mixtures of *n*/iso-paraffins were carried out (Silva and Rodrigues, 1997c) and the macropore model is solved and the simulated breakthrough curves are compared with the experimental data. Figure 7 shows the experimental and simulated adsorption/desorption curves obtained for *n*-pentane with the operating parameters compiled in Table 3. The experiments are performed in non isothermal, non adiabatic conditions. An external parabolic temperature profile is imposed ($T_o(0) = T(z = L) = 225^\circ C) T(z = 0.5L) = 253^\circ C$) to follow the experimental conditions (Silva and Rodrigues, 1997c). Desorption step is with pure nitrogen in countercurrent mode. Again, the model simulations and breakthrough runs agree fairly well. Based on these results two cyclic processes are simulated with the objective of recovering an enriched iso-pentane stream as follows:

Table 3. Operating parameters for fixed bed *n*/iso paraffins separation.

Column:			
Bed length, L,		0.20	m
Internal radius, R_w,		1.67	cm
Bed porosity, ε,		0.32	—
Feed temperature, T_0,		498.2	K
Feed pressure, P_0,		101.3	kPa
Feed superficial velocity, u_o,		0.0032	m/s
Molar feed composition,	n-C_5H_{12} (1)	9.0	%
	i-C_5H_{12} (2)	40	%
	N_2 (3)	51	%
Wall density, ρ_w,		8238	kg/m^3
Overall heat transfer, U,		15	W/m^{2}K
Wall specific heat, $\hat{C}_{pw}$,		500	J/kg K
Adsorbent: 5A zeolite.			
Pore radius, r_p,		0.17	μm
Pellet radius, R_p,		1.6	mm
Bulk density, ρ_b,		768.4	kg/m^3
Pellet void fraction, ε_p,		0.35	—
Tortuosity, τ,		1.6	—
Specific solid heat, $\hat{C}_{ps}$,		920	J/kg K

Equilibrium: Nitta model.

$$Py_i K_i = \theta_i \Big/ \left(1 - \sum_{i=1}^{n} \theta_i\right)^{s_i};\ \theta_i = n_i/m_i;\ K_i = K_{i,o}\exp\left(\frac{-\Delta H_i}{\Re T}\right)$$

Component	m_i (mol/kg)	$K_{i,o}$ (kPa^{-1})	s_i	$-\Delta H_i$ (J/mol)
n-Pentane	1.802	2.06 10^{-7}	5	55176
n-Hexane	1.509	5.03 10^{-7}	6	59356

Iso-pentane and nitrogen are considered not adsorbing.

PSA Process

A four-step PSA process based on Minkkinen et al. (1993) patent including: (i) Pressurization with feed

($Y_1 = 0.139$; $Y_2 = 0.046$; $Y_3 = 0.815$; where 1 = nC$_5$, 2 = nC$_6$ and 3 = iC$_5$); (ii) High pressure feed where the enriched iso-paraffin stream is obtained; (iii) Countercurrent blowdown step; (iv) Low pressure purge with iso-paraffin product stream. This simulation required 66 finite elements with two internal collocation points and 60 cycles to achieve the cycle steady-state, with 16 to 18 CPU minutes per cycle.

Adsorption/Desorption Process

A single two-step process supported on Holcombe et al. (1990) patent is also studied where an adsorption feed step with feed $Y_1 = 0.1$; $Y_2 = 0.05$; $Y_3 = 0.25$; $Y_4 = 0.60$; (where 4 = H$_2$) and a countercurrent purge-desorption step with feed of mole composition of $Y_1 = Y_2 = 0$; $Y_3 = 0.1$; $Y_4 = 0.9$. In this simulation nearly 40 cycles are required to reach the cyclic steady-state using 51 finite elements with two internal collocation each, spending between 8 to 10 CPU minutes for complete cycle simulated.

The main characteristics and operating conditions for both processes are reported in Table 4. High purity iso-paraffin streams are obtained with both processes; however, the Minkkinen et al. (1993) process seems to be more efficient in terms of recovery of

Table 4. Operating parameters for IFP, and UOP cycles for the *n*/iso paraffins separation.

PSA, IFP Cycle (Minkkinen et al., 1993):			
Column:			
Bed length, L,		4	m
Internal radius, R_w,		6.35	cm
Bed porosity, ε,		0.336	—
Feed temperature, T_0,		573.2	K
Molar feed composition,	n-C$_5$H$_{12}$ (1)	13.9	%
	i-C$_6$H$_{12}$ (2)	4.6	%
	i-C$_5$H$_{12}$ (3)	81.5	%
Bulk density, ρ_b,		750	kg/m^3
Overall heat transfer, U,		3.1	W/m^{2}K
Initial and other operating conditions:			
Column filled with iso-pentane, 573 (K) and 200 (kPa);			
High pressure,		1500	kPa
Low pressure,		200	kPa
Pressurization and Blowdown steps of		83	s
Feed and Vacuum Purge steps of		282	s
Load, 688 L/h kg cycle at standard conditions (273 (K), 101 (kPa)).			
Adsorption/desorption UOP Cycle (Holcombe et al., 1990):			
Column:			
Bed length, L,		4	m
Internal radius, R_w,		30	cm
Feed temperature, T_0,		533	K
Feed pressure, P_0,		1750	kPa
Molar feed composition,	n-C$_5$H$_{12}$ (1)	10	%
	n-C$_6$H$_{12}$ (2)	5	%
	i-C$_5$H$_{12}$ (3)	25	%
	H$_2$ (4)	60	%
Initial and other operating conditions:			
Column filled with iso-pentane, at 533 (K) and 1750 (kPa);			
Feed step of		135	s
Purge step of		94	s
Load, 990 L/h kg cycle at standard conditions (273 (K), 101 (kPa)).			

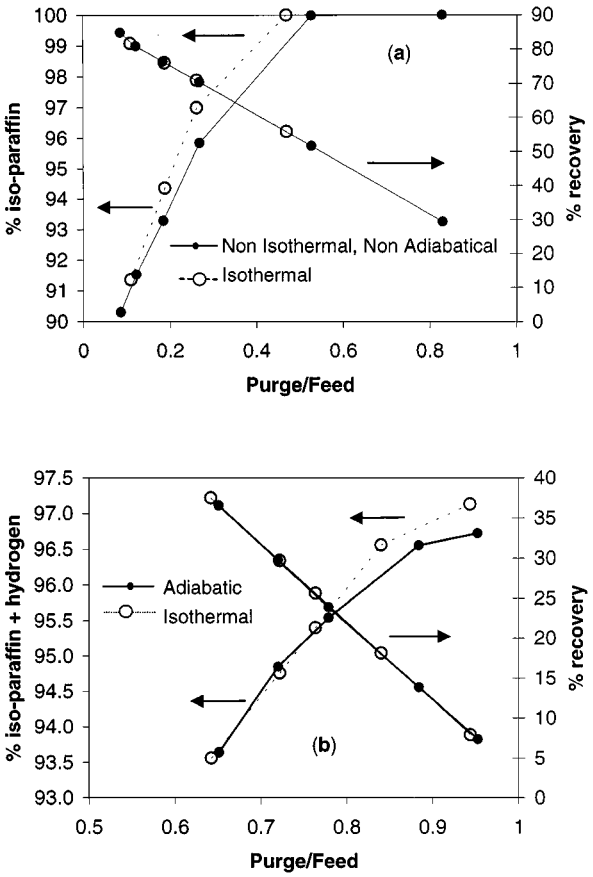

Figure 8. (a) Molar percentage of iso-paraffin and recovery of iso-paraffin as function of purge/feed molar ratio. Simulations are with non-isothermal, non-adiabatic macropore control model (IFP process). (b) Molar percentage of iso-paraffin and hydrogen and recovery of iso-paraffin and hydrogen fraction as function of purge/feed molar ratio. Simulations with adiabatic and macropore control model (UOP process). Isothermal predictions are also shown in both cases.

product for the operating conditions used in the simulation. This conclusion can be made by comparing Figs. 8(a) and (b) where purity-recovery versus the purge to feed molar ratio are shown for both cases. The desorption effluent drawn off reported by Minkkinen et al. (1993) has an averaged value of 27% mole on nC$_5$ and 7.5% on nC$_6$ while the simulated values obtained are 23.2 and 7.6% for purge step, respectively. Holcombe et al. (1990) reports a product with approximately 98% on iso paraffins and H_2, while the simulated values are between 96 and 97%. In both cases, the simulated average values for molar concentrations are near to the expected results reported on the commercial patents.

Conclusions

A versatile simulator package based on simple models has been developed and tested in two cyclic adsorptive separations: the propylene/propane system and *n*/iso paraffins mixtures. Experimental breakthrough data from both systems were compared with the simulated results showing reasonable agreement. The simulated predictions for the propylene/propane system using two different approaches, namely a three-step TSA process and a four-step VSA process, establishes that it is possible to obtain a high propylene product from an equimolar mixture but with a low recovery using an adsorbent commercial available. For the *n*/iso-paraffin system a high iso-paraffin or a iso-paraffin + H_2 product is obtained in both cyclic processes analyzed, although in terms of recovery the four-step PSA process is more efficient.

Nomenclature

a	specific pellet area, $(=3/R_p)$	m^{-1}
$Bi_{m,i}$	mass Biot number	—
$\bar{c}_i$	average mole concentration of "i" component in the pellet	mol/m^3
C_i	mole concentration of "i" component in the bulk, CY_i	mol/m^3
C_o	total mole concentration at the feed condition	mol/m^3
$\tilde{C}_{pg}$	molar specific heat at constant pressure of the gas mixture	J/mol K
$\hat{C}_{ps}$	specific heat of the pellet	J/kg K
$\hat{C}_{pg}$	specific heat per kilogram of gaseous mixture	J/kg K
$\hat{C}_{pw}$	wall specific heat	J/kg K
$\tilde{C}_{vg}$	molar specific heat at constant volume of the gas mixture	J/mol K
d_p	spherical pellet diameter, $(=2R_p)$	m
$\bar{D}_{c,i}$	crystal diffusion coefficient for "i" component	m^2/s
$\bar{D}_{p,i}$	pore diffusivity for "i" component	m^2/s
$D_{oc,i}$	zero coverage crystal diffusion coefficient for "i" component	m^2/s
λ	heat axial dispersion coefficient	W/m K
$D_{zm,i}$	mass axial dispersion coefficient for "i" component	m^2/s
h_f	film heat transfer coefficient between gas and solid	W/m^2 K

h_w	film heat transfer coefficient between gas and the wall	W/m^2 K
$-\Delta H_i$	isosteric heat adsorption of the "i" component	J/mol
k_i	equilibrium parameter for "i" component	kPa^{-1}
$K_{m,i}$	external mass transfer coefficient for "i" component	m/s
L	length of fixed-bed	m
m_i	equilibrium parameter for "i" component	mol/kg
$\bar{\bar{n}}_i$	average adsorbed concentration for "i" component in the pellet	mol/kg
n_i^*	adsorbed phase concentration in the crystal in equilibrium with the gas inside the particle	mol/kg
N, N_i	total mass flux and mass flux for the "i" component from gas phase to solid boundary	mol/m^3 s
P	gas pressure	kPa
P_i	partial pressure of "i" component	kPa
r_c	crystal radius	m
$\Re$	ideal gas constant (=8.3144)	J/mol K
r_p	pore radius	m
R_p	equivalent spherical pellet radius	m
t	time	s
T	temperature	K
T_g	gas temperature	K
T_s	solid temperature	K
T_w	wall temperature	K
T_∞	ambient temperature	K
u	superficial gas velocity	m/s
u_o	superficial gas velocity at the feed conditions	m/s
U	overall heat transfer coefficient	W/m^2 K
Y_i	mole fraction of "i" component in the bulk	—
z	axial position	m
w_c	crystal weight fraction of the pellet	—

Greek Letters

α_w	ratio of the internal surface area to the volume of the column wall	m^{-1}
$\alpha_{w\ell}$	ratio of the log mean surface to the volume of column wall	m^{-1}
ε	interparticle void fraction of bed	—
ε_p	pellet void fraction	—
ε_w	volume wall to bed volume ratio	—
ρ_p	pellet density	kg/m^3
ρ_w	wall density	kg/m^3
μ	gas viscosity of the mixture	kg/m s
τ	tortuosity factor	—

Superscripts

$*$	equilibrium
o	pure component
$\bar{}$	volumetric average
$=$	double volumetric average
$\sim$	per mol
$\wedge$	per kilogram

Subscripts

c	crystal
g	gas
h	heat
i,j	"i" or "j" component
o	reference condition
m	mass
p	pellet; constant pressure
s	solid
v	constant volume
w	wall
z	axial coordinate
∞	external

Acknowledgments

Financial support from PRAXIS XXI /3/3.1/CEG/2644/95 is gratefully acknowledged. One of us (F.A. Da Silva) acknowledges research fellowship from PRAXIS XXI/BD5772/95).

References

Arumugam, B.K. and P.C. Wankat, "Pressure Behaviour During the Loading of Adsorption Systems," *Fundamentals of Adsorption*, M.D. LeVan (Ed.), Kluwer Academic Publishers, Boston, Massachusetts, 1996.

Bird, R.B., W.E. Stewart, and E.N. Lightfoot, *Transport Phenomena*, Wiley, New York, 1960.

Brandani, S., J. Hufton, and D. Ruthven, "Self-Diffusion of Propane and Propylene in 5A and 13X Zeolite Crystals Studied by the Tracer ZLC Method," *Zeolites*, **15**, 624 (1995).

Brown, P.N., A.C. Hindmarsh, and L.R. Petzold, "Using Krylov Methods in the Solution of Large-Scale Differential-Algebraic Systems," *SIAM J. Sci. Comput.*, **15**, 1467 (1994).

Carey, G.F. and B.A. Finlayson, "Orthogonal Collocation on Finite Elements," *Chem. Eng. Sci.*, **30**, 587 (1975).

Cen, P.L. and R.T. Yang, "Zeolite PSA Cycles for Producing a High-Purity Hidrogen from a Hydrogen-Lean Mixture," *Chem. Eng. Comm.*, **78**, 139 (1989).

Chlendi, M.W., "Séparation de gaz par adsorption modulée en pression (PSA)," Ph.D. Thesis, Ins. Nat. Poly. Lorraine, Nancy, France, 1993.

Da Silva, F.A., E.A. Macedo, and A.E. Rodrigues, "Computer Aided Process Design and Optimization with Novel Separation Process," JOU2-CT93-0337, Final Report, January–July 1996.

Huang, C.C. and J.R. Fair, "Study of the Adsorption and Desorption of Multiple Adsorbates in a Fixed Bed," *AIChE J.*, **34**, 1861 (1988).

Huang, Y.H., J.W. Johnson, A.I. Liapis, and O.K. Crosser, "Experimental Determination of Binary Equilibrium Adsorption and Desorption of Propane-Propylene Mixtures on 13X Molecular Sieves by a Differential Sorption Bed System and Investigation of Their Equilibrium Expressions," *Sep. Technol.*, **4**, 156 (1994).

Holcombe, T.C., "Isomerization Process," U.S. Patent, 4,210,771, 1980.

Holcombe, T.C., T.C. Sager, W.K. Volles, and A.S. Zarchy, "Isomerization Process," U.S. Patent 4,929,799, 1990.

Järvelin, H., "Adsorption of Propane and Propylene," SRP Doc., No. F-90-4, Separations Research Program, The University of Texas at Austin, 1990.

Järvelin, H. and J.R. Fair, "Adsorptive Separation of Propylene-Propane Mixtures," *Ind. Eng. Chem.*, **32**, 2201 (1993).

Kumar, R., T.C. Golden, T.R. White, and A. Rokicki, "Novel Adsorption Distillation Hybrid Scheme for Propane/Propylene Separation," *Sep. Technol.*, **15**, 2157 1992.

Kumar, R., V.G. Fox, D.G. Hartzog, R.E. Larson, Y.C. Chen, P.A. Houghton, and T. Naheiri, "A Versatile Process Simulator for Adsorptive Separations," *Chem. Eng. Sci.*, **49**, 3115 (1994).

LaCava, A., J.A. Dominguez, and J. Cardenas, "Modeling and Simulation of Rate Induced PSA Separations," *Adsorption: Science and Technology*, A.E. Rodrigues, M.D. LeVan, and D. Tondeur (Eds.), NATO ASI Ser., vol. 158, pp. 323, 1989.

Liu, Y and J.A. Ritter, "Pressure Swing Adsorption-Solvent Vapor Recovery: Process Dynamics and Parametric Study," *Ind. Eng. Chem. Res.*, **35**, 2299 (1996).

Lu, Z.P., J.M. Loureiro, M.D. LeVan, and A.E. Rodrigues, "Simulation of a Three-Step One-Column Pressure Swing Adsorption Process," *AIChE J.*, **39**(9), 1483 (1993).

Malek, A. and S. Farooq, "Study of a Six-Bed Pressure Swing Adsorption Process," *AIChE J.*, **43**, 2509, (1997).

Minkkinen, A., L. Mank, and S. Jullian, "Process for the Isomerization of C5/C6 Normal Paraffins with Recycling of Normal Paraffins," U.S. Patent 5,233,120, 1993.

Myers, A.L. and J.M. Prausnitz, "Thermodynamics of Mixed-Gas Adsorption," *AIChE J.*, **11**, 121 (1965).

Nitta, T., T. Shigetomi, M. Kurooka, and T. Katayama, "An Adsorption Isotherm of Multi-site Occupancy Model for Homogeneous Surface," *J. Chem. Eng. Jpn.*, **17**, 39 (1984).

Park, I., D.D. Do, and A.E. Rodrigues, "Measurement of the Effective Diffusivity in Porous Media by the Diffusion Cell Method," *Catal. Rev. Sci. Eng.*, **38**, 189 (1996).

Reid, R.C., J.M. Prausnitz, and B.E. Poling, *The Properties of Gases and Liquids*, 4th Edition, McGraw-Hill, NY., USA, 1987.

Schiesser, W.E., *The Numerical Method of Lines*, Academic Press, California, USA 1991.

Schork, J.M. and J.R. Fair, "Parametric Analysis of Thermal Regeneration of Adsorption Beds," *Ind. Eng. Chem. Res.*, **27**, 457 (1988).

Sikavitsas, V.I., R.T. Yang, M.A. Burns, and E.J. Langenmayr, "Magnetically Stabilized Fluidized Bed for Gas Separations: Olefin-Paraffin Separations by π-Complexation," *Ind. Eng. Chem. Res.*, **34**, 2873 (1995).

Silva, J.A. and A.E. Rodrigues, "Sorption and Diffusion of *n*-pentane in Pellets Zeolite 5A," *Ind. Eng. Chem. Res.*, **36**, 493 (1997a).

Silva, J.A. and A.E. Rodrigues, "Sorption and Diffusion of *n*-Hexane in Pellets Zeolite 5A," *AIChE J.*, **43**, 2524 (1997b).

Silva, J.A. and A.E. Rodrigues, "Fixed-Bed Adsorption of *n*-Pentane/Isopentane Mixture in Pellets of 5A Zeolite," *Ind. Eng. Chem. Res.*, **36**, 3769 (1997c).

Sircar, S., "Excess Properties and Thermodynamics of Multicomponent Gas Adsorption," *J. Chem. Soc., Faraday Trans.*, **81**(1), 1527–1540 (1985).

Sircar, S., "Isosteric Heats of Multicomponent Gas Adsorption on Heterogenenous Adsorbents," *Langmuir*, **7**, 3065 (1991).

Talu, O., J. Li, and A.L. Myers, "Activity Coefficients of Adsorbed Mixtures," *Adsorption*, **1**, 103 (1995).

Tidball, J.F., P.S. Ward, and F.A. Perris, "The Simulation of Industrial Adsorption Processes," *Gas Separation Technology*, E.F. Vansant and R. Dewolfs (Eds.), p. 75, Elsevier Science Publishers, B.V., Netherlands, 1989.

Villadsen, J. and M.L. Michelsen, *Solution of Differential Equation Models by Polynomial Approximation*, Prentice-Hall, Englewood Cliffs, NJ, 1978.

Wakao, N. and T. Funazkri, "Effect of Fluid Dispersion Coefficients on Particle-to-Fluid Mass Transfer Coefficients in Packed Beds," *Chem. Eng. Sci.*, **33**, 1375 (1978).

Wakao, N. and B.H. Chen, "Some Models for Unsteady-state Heat Transfer in Packed Bed Reactors," *Recent Trends in Chemical Reaction Engineering*, B. Kulkarni, R. Mashelkar and M. Sharma (Eds.), vol. 1, p. 254, Wiley Eastern Ltd., New Delhi, 1987.

Yang, R.T. *Gas Separation by Adsorption Processes*, Butterworths, USA, 1987.

Yang, R.T. and E.S. Kikkinides, "New Sorbents for Olefin-Paraffin Separations by Adsorption via π-complexation," *AIChE J.*, **41**, 509 (1995).